INTERNATIONAL JOURNAL OF PRECISION ENGINEERING AND MANUFACTURING Vol. 15, No. 7, pp. 1405-1410 JULY 2014 / 1405
DOI: 10.1007/s12541-014-0483-x

Numerical Investigation on the Effects of the Positional Variation of Porosity in Thin Porous Layers

Taqi Ahmad Cheema[1], Choon-Young Lee[1], Gyu-Man Kim[1], Jung-Goo Hong[1], Moon-Kyu Kwak[1], and Cheol-Woo Park[1,#]

1 School of Mechanical Engineering, Kyungpook National University, 1370 Sankyuk-dong, Buk-gu, Daegu, South Korea, 702-701
Corresponding Author / E-mail: chwoopark@knu.ac.kr, TEL: +82-53-950-7569, FAX: +82-53-950-6550

KEYWORDS: Porosity, Positional variation, Numerical simulation, Composite porous layer, Wall region, Central region

The application of pressure in the assembly of devices containing thin porous layers has shown significant effects with the presence of a solid boundary contact. During this process, pore diameters of the thin porous layers are reduced. Thus, the porosity in the near wall region is effectively reduced. The reduced porosity significantly lowers the overall performance of the devices because of the limited fluid dynamic variables. A new method for the positional variation of porosity is proposed to compensate the fluid dynamic disadvantages and mass transport characteristics in the industrial devices such as filters, porous electroosmotic pump and fuel cells. In the present study, the novel method introduces a composite porous layer with high porosity in the outer region rather than in the central region of the porous media. A three-dimensional numerical simulation is performed to investigate the effects of this positional variation of porosity and the performance of the composite porous layer. A reasonable increase in flow rate is found in the wall region and in the central region, depending on the increment in the porosity in the outer region and on the orientation of the porous layer to the fluid flow.

Manuscript received: March 11, 2013 / Revised: March 11, 2014 / Accepted: March 17, 2014

NOMENCLATURE

c = Concentration of tracer
D = Diffusion coefficient
k = Permeability of porous layer
p = Pressure of fluid
$\vec{N}$ = Flux vector
$\vec{V}$ = Fluid velocity vector
ρ = density of fluid
μ = viscosity of fluid
ε = porosity of porous layer

1. Introduction

The use of porous media in various industrial power and energy applications has been a prominent research topic for the past three decades. Studies conducted in the past primarily focused on developing theories related to porous media. This research focus has recently shifted to the performance enhancement of industrial applications that use porous media. This performance enhancement has been implemented by a detailed study of porous media parameters, which includes porosity, permeability, morphological and geometrical configurations, thermal dispersion, and local thermal non-equilibrium properties. In 1856, Henry Darcy proposed the proportionality between velocity and pressure gradient, which was later experimentally verified by numerous researchers.[1]

The Darcy law primarily became the starting point for investigations on fluid flow and heat transfer through porous media. Darcy's equation was found to be valid for flows with pressure gradient as the major driving force. As for the momentum transfer, the viscous effects were neglected. Therefore, using Darcy law as the only equation to solve a porous medium was restricted by several limitations, as reported by numerous authors.[2-4] The studies of these authors focused on incorporating the inertial and solid boundary effects in the Darcy equation to implement it especially in small systems. Brinkman[5] extended the Darcy law and added another viscous transport term to the momentum equation by treating pressure and velocity vectors as dependent variables. This extension made it possible to combine the

subdomains of free flow with the subdomains of porous media flow.

In porous subdomains, the flow variables and the fluid properties are averaged over a control volume surrounding a point. Porosity is defined as the fraction of the control volume occupied by the pores, and the value varies from 0 to 1 for pure solid regions and for subdomains of free flow, respectively. This parameter is highly significant when dealing with the physics of porous media. Several other studies in the past considered constant porosity for a whole porous medium.[6-9] Kaviany used the Brinkman extended flow model with a constant porosity matrix for the flow through parallel plates.[10] However, the porosity variation near the solid boundary was later found to have a significant effect on the velocity fields in packed beds, a phenomenon termed as the channeling effect. Several experimental and numerical studies for flow and heat transfer through porous media considered variable porosity and used a variable porosity function to model such variations.[11-13]

Several of the recently developed industrial applications such as fuel cell and electroosmotic pumps, which use very thin porous layers, are facing highly significant effects of the presence of solid boundary.[14,15] The application of pressure in the assembly of such devices reduces pore diameter, thus reducing the porosity in the wall region. Moreover, the elastic deformation of the porous layers as a result of fluid dynamic loading is also another important factor altering the constant porosity distribution. This phenomenon is commonly known as the fluid-structure interaction and it can be frequently observed in a filtration process where the reduction in porosity of filtration medium highly depends on its orientation to the fluid flow.[16,17] When the porosities in the near wall region are reduced, overall performance of the devices using thin porous layers is greatly decreased with substantial variations in fluid dynamic characteristics and mass transport features. Therefore, there need to compensate those loss of porosities to improve the device performance intactly by enhancing the flow and mass transport properties in the reduced porosity region.[18]

In the present study, we propose the advanced application of thin composite porous layers by numerically investigating their flow and mass transfer abilities, while placing them in two different orientations (i.e., parallel and perpendicular to the flow direction). The reduced flow and mass transfer in the porous layers can be restored by introducing a high porosity in the outer region rather than in the central region. A three-dimensional simulation is performed to investigate the effects of this newly proposed method of porosity variation in this study. Two different orientations (i.e., parallel and perpendicular to the flow direction) of the porous media in a micro-channel are numerically simulated to investigate the physics of the flow and mass transport through the porous matrix. First, the physics of free and porous media flow is simulated based on the coupling between the Navier-Stokes and Brinkman equations to determine the effects of porosity variation on flow variables in the porous matrix. The results of the first study are then coupled to transient simulation to investigate the effects on species transport.

2. Model Development and Mathematical Modeling

Two cases of 10-μm thick porous layers with two different orientations in the flow field were used in the study. Fig. 1(a) shows a three-dimensional rectangular channel with the porous layer at the top with cross section of 10 μm × 100 μm. The cross section of the channel measured was 100 μm × 100 μm having a length of 2000 μm. Fig. 1(b) shows a three-dimensional cylindrical tube measuring 100 μm in diameter and containing 10-μm thick porous layer placed perpendicular to the flow direction at 1000 μm from the channel inlet.

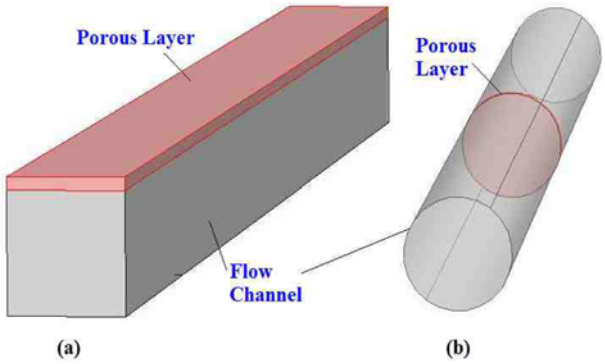

Fig. 1 General computational models used in the study: (a) porous layer parallel to the flow direction; (b) porous layer perpendicular to the flow direction

2.1 Free flow modeling

The flow domain was assumed to contain a single-phase fluid. The effect of external force, compressibility, and gravitational effects were neglected, and a laminar fluid flow was considered. The governing equations for this fluid flow are Navier-Stokes equations given below.

Mass conservation equation:

$$\nabla \cdot \vec{V} = 0 \tag{1}$$

Momentum conservation equation:

$$\rho(\vec{V} \cdot \nabla)\vec{V} = -\nabla p + \mu\nabla(\nabla\vec{V} + (\nabla\vec{V})^T) \tag{2}$$

where ρ is the fluid density, $\vec{V}$ is the velocity vector, p denotes the pressure, and μ is the fluid viscosity.

At the inlet, a laminar inflow velocity of 100 μm/s was introduced. Outlet boundary conditions were fixed to laminar atmospheric boundary conditions. The channel domain walls had a no-slip boundary condition.

2.2 Porous Media Modeling

Fluid flow in the porous media can be modeled either by the Darcy law or by the Brinkman equation. Darcy law is not valid for flow where viscous effects are important. Therefore, in this study, steady flow in the porous media was modeled using the Brinkman equation, neglecting the effects of external forces and source/sink terms.

$$\nabla \cdot \vec{V} = 0 \tag{3}$$

$$\frac{\mu}{k}\vec{V} = -\nabla p + \mu\nabla(\nabla\vec{V} + (\nabla\vec{V})^T) \tag{4}$$

where k represents the permeability of the porous material.

The Brinkman formulation makes it possible to account for viscous

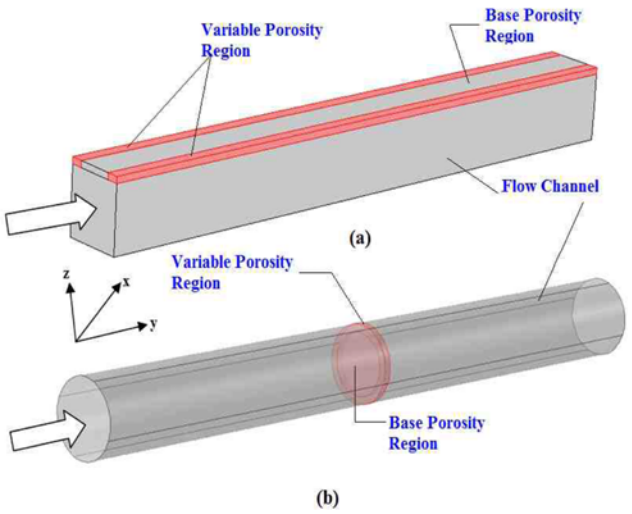

Fig. 2 Computational models with variable porosity regions: (a) porous layer parallel to the flow direction; (b) porous layer perpendicular to the flow direction

effects and for the flow variables as dependent variables. The walls of the porous media were subjected to symmetrical boundary conditions.

2.3 Mass Transport Modeling

A tracer specie was injected into the channel to investigate transient mass transport effects in the composite thin porous layer, assuming that the specie does not influence the porous structure. Mass transport is governed by the following equation:

$$\frac{\partial c}{\partial t}+\nabla\cdot\vec{N}=0 \tag{5}$$

where c denotes the tracer concentration, and $\vec{N}$ is the flux vector that can be defined by the Nernst-Planck equation;

$$\vec{N}=-D\nabla c+c\vec{V} \tag{6}$$

where D represents the diffusion coefficient.

The inlet and outlet of the channel were assigned flux conditions to set the diffusion and convection contribution. The walls of the porous media were set with symmetry boundary conditions.

3. Numerical Method and Implementation

First, both domains were solved for free flow with a porosity value of 1 in the porous matrix to estimate a reduced velocity region. The reduced velocity region was found approximately 20 and 10 μm away from the walls of the parallel porous layer and of the perpendicular porous layer, respectively. Based on this estimation, the porous media was divided broadly into two regions: constant base porosity (i.e., central region) and variable porosity (i.e., near wall region). The two new slots introduced outside the maximum velocity region were assigned with higher porosity ranging from 0.4 to 0.9 compared with the central region with a base porosity value of 0.4.

In this study, we used the commercial software COMSOL-Multiphysics that uses the finite element method to solve equations.

Table 1 Parameters used in the numerical study

Parameter	Symbol	Value
Density	ρ	1.2 kg/m^3
Viscosity	μ	1E-05 Pa-s
Permeability	k	1E-11 m^2
Diffusion Coefficient	D	1E-09 m^2/s

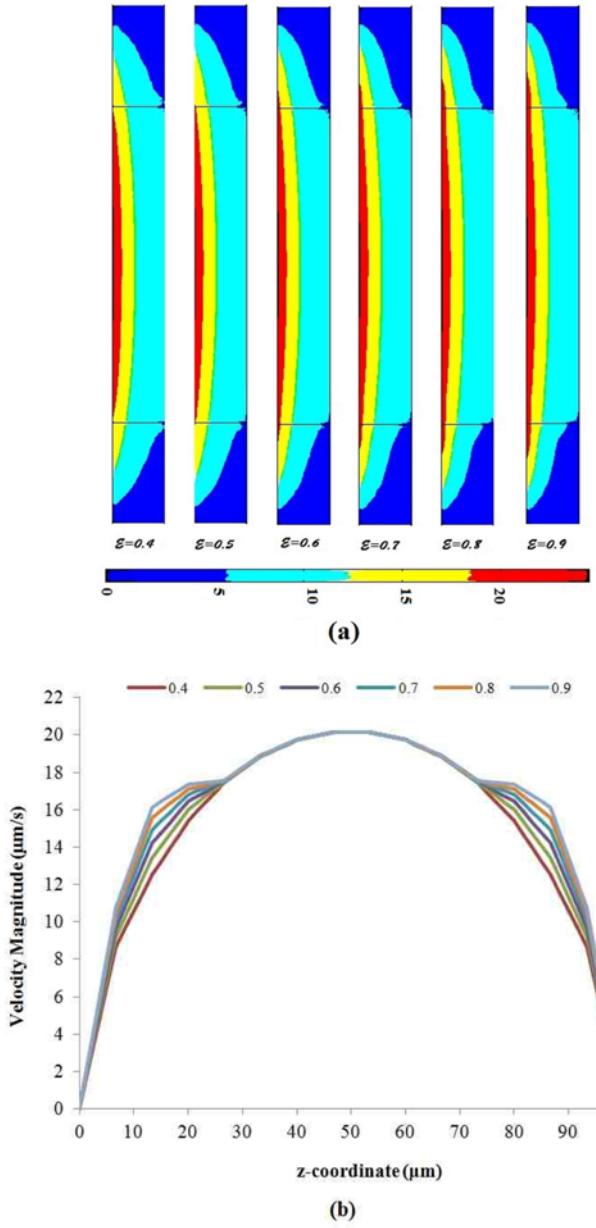

Fig. 3 Simulation results for the porous layer parallel to the flow direction: (a) velocity slice plots (unit: μm/s); (b) graphical plot at the channel-porous layer interface

The two distinct physics for the flow in the channel and the porous media were coupled for a steady-state simulation using a combined free and porous media flow application mode available in the commercial code. The computational domain of the parallel porous layer model was discretized using mapped meshing with 7500 elements; 35,465 degrees of freedom were solved. Solving for the computational domain took 22 seconds using a 2.93 GHz computer processor. For the perpendicular

porous layer model, free tetrahedral mesh discretized the computational domain with 103,701 mesh elements. The total number of degrees solved was 82,508 in 36 seconds. In each case, an iterative generalized minimal residual solver was used for 1000 iterations with a tolerance factor of 1E-3.

In the second stage of the study, a time-dependent numerical simulation was implemented to investigate the species concentration by using the steady-state velocity field from the first stage. In each geometrical configuration and porosity value, the solution ran for 2 seconds with an interval of 0.1 second.

4. Results and Discussion

4.1 Effects on the velocity in the porous layer

Fig. 3(a) shows the velocity slice plot for a thin porous layer placed parallel to the flow direction on top of a square channel. The plot shows that increasing the porosity in the near wall region increases the flow rate in that region and the velocity magnitude in the central region. The increased porosity in the near wall region also affects the central region of the porous layer and will eventually enhance the performance of the device in which such porosity variations are introduced. This increased porosity will also compensate for the effect of porosity reduction resulting from external pressure or any other effect near the boundary region. Fig. 3(b) shows the graphical plot for the velocity magnitude on the channel-porous layer interface. The graph elaborates in detail the results shown by slice plots. The clear effect of porosity variation starts 5 μm away from the wall and peaks near the central region. For each integer increase in porosity, the maximum increase in the velocity magnitude found is approximately 1 μm/s considering 100 μm/s inlet velocity. This increase has significant effects on the enhancement of device performance.

Fig. 4(a) shows the velocity slice plot for the thin porous layer placed perpendicular to the flow direction in a cylindrical channel. The plot shows an overall increase in the flow rate because of the position of the porous media in the main flow stream. However, the pattern of increasing velocity is similar to the case of parallel porous media, excluding the central region. The central region is affected by porosity variation in the outer region with a slightly decreased velocity compared with the case with a base porosity value of 0.4.

Fig. 4(b) shows the graphical plot for the velocity magnitude on the leading porous layer interface. The graph elaborates in greater detail a similar pattern of results shown by the slice plots. It also shows that the clear effect of porosity variation starts 2 μm away from the wall and peaks near the central region. For each integer rise in porosity, the maximum increase in the velocity magnitude found is approximately 1 μm/s considering an inlet velocity of 100 μm/s. This increase can have significant effects on the enhancement of device performance. The effect of increased porosity in the near wall region for perpendicularly placed porous layers is more important and can reduce the viscous effects in the near wall region. In-depth studies on increased porosity in particular application areas are thus needed.

4.2 Effects on shear rate in the porous layer

The difference between the Brinkman equation and the Darcy law

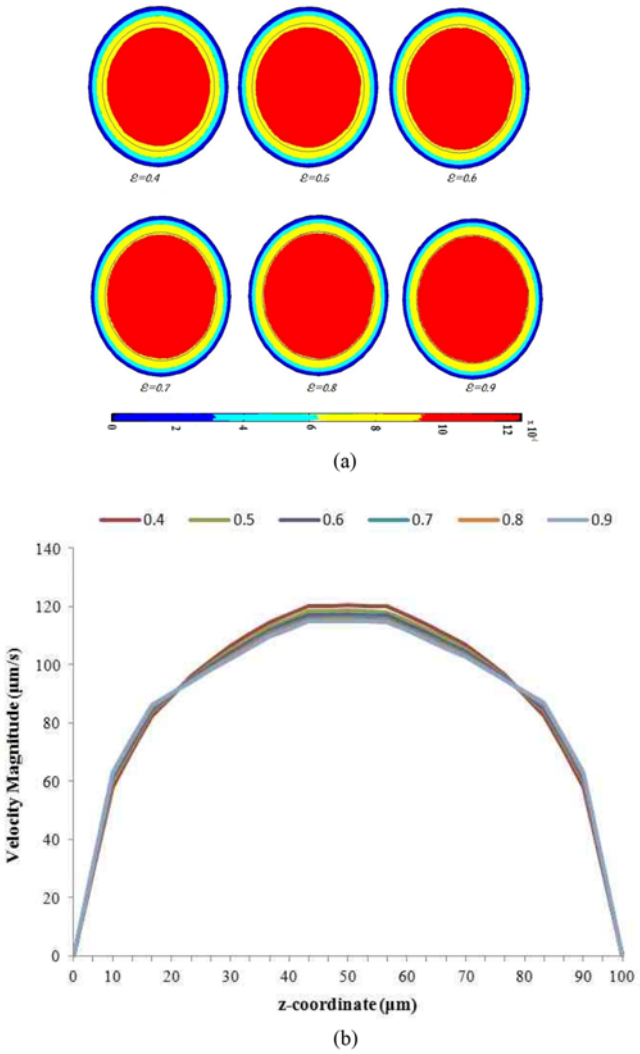

Fig. 4 Simulation results for the porous layer perpendicular to the flow direction: (a) velocity slice plots (unit: μm/s); (b) graphical plot at the leading porous layer interface

is the viscous transport in the momentum balance. Therefore, studying the shear rate in porous media resulting from the porosity variation in the near wall region is highly important. Fig. 5(a) shows the shear rate variation across the channel-porous layer interface for the case of the parallel porous layer. The graphical plot shows a gradual decrease in shear rate of up to 5 μm starting from the wall followed by an approximate linear rise until the end of the outer region. This linear rise then sharply drops in the central region, resulting in an average rise of 1/s shear rate. This high shear rate value shows the importance of porosity variation in the near wall region. Fig. 5(b) shows the shear rate variation at the leading interface of the porous layer for the case of the perpendicular porous layer. The shear rate drops sharply almost at the same rate in most outer regions, but maintains a consistent difference of approximately 0.20 per second before and after the outer and central region interfaces.

4.3 Effects on species transport in the porous layer

Fig. 6(a) shows the graphical plot for the total flux magnitude on the channel-porous layer interface. The graph looks similar to the plot of

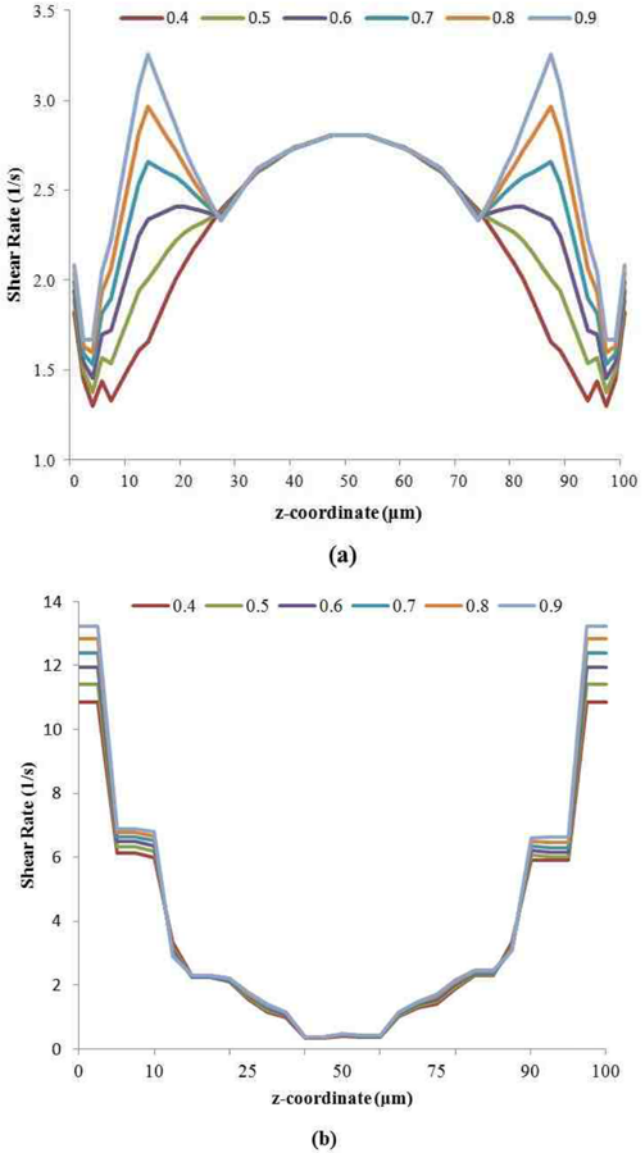

Fig. 5 Shear rate plots at the porous layer interface: (a) porous layer parallel to the flow direction; (b) porous layer perpendicular to the flow direction

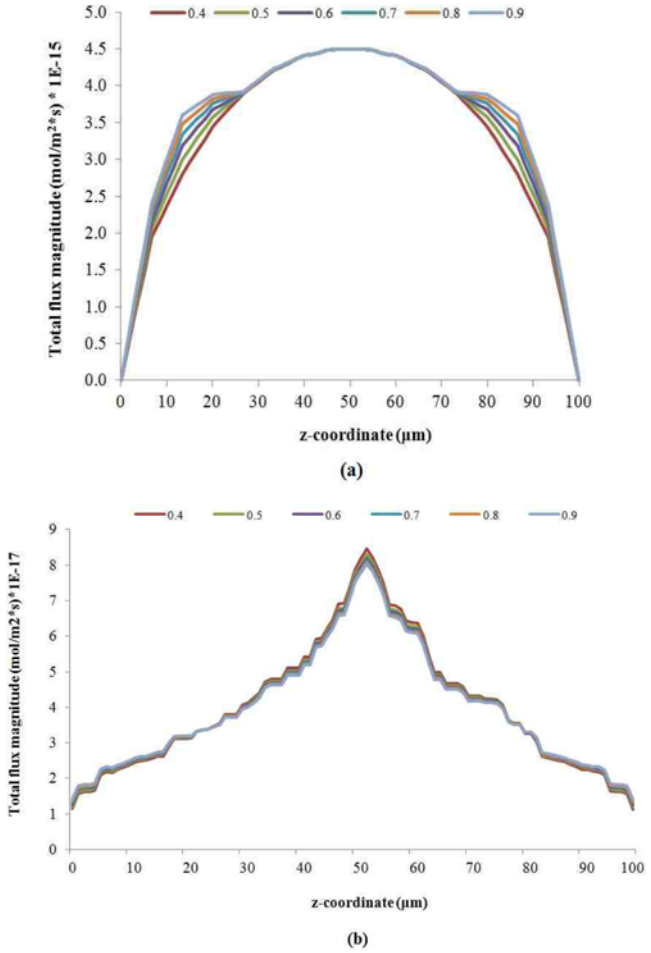

Fig. 6 Graphical plot for the total flux magnitude of species: (a) parallel porous layer; (b) perpendicular porous layer

velocity magnitude for the parallel porous layer, which shows the effect of increased flux magnitude in the outer region of the porous matrix and in the adjacent central region. Mass transport in such a composite porous layer can be predicted by the velocity magnitude pattern. However, the scale of the total flux magnitude indicates that this increase is very small compared with the increase in the velocity magnitude. The increase in flux becomes significant initially after 10 μm and continues to increase within 10 μm of the central region. This increase can have significant effects on the enhancement of device performance.

Fig. 6(b) shows the graphical plot for the total flux magnitude in the front porous layer interface of the perpendicularly placed porous media in the tube. The graph elaborates a similar pattern of results for all the porosity values. However, the flux magnitude slightly increases with increasing porosity in outer region and continues to increase in the neighboring central region. This increase, however, is compensated in the central region where the flux magnitude for different porosity cases decreases with the same margin as that of the increase in the outer region. The porosity variation in the thin porous layer placed perpendicular to the flow direction does not significantly affect species transport.

5. Conclusion

A numerical study was carried out addressing the issue of reduced porosity of thin porous layers adjacent to the solid wall because of the application of pressure during the assembly process. This study emphasizes the need for a composite porous layer with higher porosity in the near wall region than in the central region. A significant increase in velocity magnitude was observed in the near wall region and in the central region for the two cases classified according to the placement of porous layers with respect to flow direction. However, the perpendicularly placed thin porous layer may not have significant effects from such porosity variation, as the flow rate in the central region decreases with the same amount. These effects were also verified by shear plots at the channel-porous layer interface. In the present study, we focused on the evaluations of the fluid dynamic characteristics and mass transport features with application of newly

proposed method of positional variation in thin composite porous layers. Consequently, various industrial devices can be applicable to these composite porous layers to enhance their performances such as flow filters, porous electroosmotic pump and fuel cell etc. Such performance enhancement was evident in species transport, producing results similar to those presented in the velocity magnitude.

ACKNOWLEDGMENTS

This work was supported by a Korea Research Foundation (KRF) grant funded by the Korean Government (MEST) (No. 2012R1A2A2A 01046099, 2011-0023437), and a grant from the Priority Research Centers Program through the National Research Foundation of Korea (NRF) funded by the Ministry of Education, Science and Technology (2012-0005856).

REFERENCES

1. Nield, D. A. and Bejan, A., "Convection in Porous Media," Springer, 3rd Ed., pp. 6-14, 2006.
2. Chandrasekhara, B., "Flow Model for Velocity Distribution in Fixed Porous Beds under Isothermal Conditions," Thermo and Fluid Dynamics, Vol. 12, No. 2, pp. 105-111, 1979.
3. Vafai, K. and Tien, C., "Boundary and Inertia Effects on Flow and Heat Transfer in Porous Media," International Journal of Heat and Mass Transfer, Vol. 24, No. 2, pp. 195-203, 1981.
4. Bejan, A. and Poulikakos, D., "The Nondarcy Regime for Vertical Boundary Layer Natural Convection in a Porous Medium," International Journal of Heat and Mass Transfer, Vol. 27, No. 5, pp. 717-722, 1984.
5. Brinkman, H. C., "A Calculation of the Viscous Force Exerted by a Flowing Fluid on a Dense Swarm of Particles," Applied Scientific Research, Vol. 1, No. 1, pp. 27-34, 1949.
6. Poulikakos, D. and Kazmierczak, M., "Forced Convection in a Duct Partially Filled with a Porous Material," Journal of Heat Transfer, Vol. 109, No. 3, pp. 653-662, 1987.
7. Sung, H. J., Kim, S. Y., and Hyun, J. M., "Forced Convection from an Isolated Heat Source in a Channel with Porous Medium," International Journal of Heat and Fluid Flow, Vol. 16, No. 6, pp. 527-535, 1995.
8. Nield, D. A., Junqueira, S. L. M., and Lage, J. L., "Forced Convection in a Fluid-Saturated Porous-Medium Channel with Isothermal or Isoflux Boundaries," Journal of Fluid Mechanics, Vol. 322, pp. 201-214, 1996.
9. Chen, S. C. and Vafai, K., "Analysis of Free Surface Momentum and Energy Transport in Porous Media," Numerical Heat Transfer, Part A Applications, Vol. 29, No. 3, pp. 281-296, 1996.
10. Kaviany, M., "Laminar Flow through a Porous Channel Bounded by Isothermal Parallel Plates," International Journal of Heat and Mass Transfer, Vol. 28, No. 4, pp. 851-858, 1985.
11. Vafai, K., "Convective Flow and Heat Transfer in Variable-Porosity Media," Journal of Fluid Mechanics, Vol. 147, pp. 233-259, 1984.
12. Vafai, K., Alkire, R. L., and Tien, C. L., "An Experimental Investigation of Heat Transfer in Variable Porosity Media," Journal of Heat Transfer, Vol. 107, No. 3, pp. 642-647, 1985.
13. Poulikakos, D. and Renken, K., "Forced Convection in a Channel Filled with Porous Medium, including the Effects of Flow Inertia, Variable Porosity, and Brinkman Friction," Journal of Heat Transfer, Vol. 109, No. 4, pp. 880-888, 1987.
14. Roshandel, R., Farhanieh, B., and Saievar-Iranizad, E., "The Effects of Porosity Distribution Variation on PEM Fuel Cell Performance," Renewable Energy, Vol. 30, No. 10, pp. 1557-1572, 2005.
15. Ling, Z., Yang, T., Meng, F. C., Yi, L., and Zhang, X. X., "Simulation and Experimental Study of a Porous Electroosmotic Pump," Key Engineering Materials, Vol. 483, pp. 320-326, 2011.
16. Iliev, O., Mikelic, A., and Popov, P., "On Upscaling Certain Flows in Deformable Porous Media," Multiscale Modeling & Simulation, Vol. 7, No. 1, pp. 93-123, 2008.
17. Andrä, H., Iliev, O., Kabel, M., Kirsch, R., Lakdawala, Z., and Ricker, S., "FluidStructure Interaction in Porous Media for Loaded Filter Pleats," PAMM, Vol. 11, No. 1, pp. 489-490, 2011.
18. Roshandel, R. and Farhanieh, B., "The Effects of Non-Uniform Distribution of Catalyst Loading on Polymer Electrolyte Membrane Fuel Cell Performance," International Journal of Hydrogen Energy, Vol. 32, No. 17, pp. 4424-4437, 2007.